

**Online supplement for the manuscript 'Progesterone and HMOX-1 promote fetal growth by CD8<sup>+</sup>T cell modulation' by Solano ME et al.,**

**Supplemental Materials and Methods**

*Magnetic resonance imaging (MRI)*

Placental L/Jz ratio: formalin fixed and Gadolinium treated placentas were placed in 1% agarose gel. Imaging of the specimen in the tube was performed on a 7T animal scanner (ClinScan, Bruker). 3D data were acquired using a T1-weighted turbo spin echo sequence (90° flip-back pulse (RESTORE), TR: 200ms, TE: 18ms, turbo factor 8, number of signal averages 2, oversampling 50%, acquisition time: 42min, FoV: 36mm x 36mm x 7.68mm, matrix: 448 x 448 x 96, voxel size: 80 µm). To generate the L/Jz ratio, the volume of the placental functional zones was measured in three mid-sagittal images of each placenta at the level of the umbilical cord.

Identification of high perfusion zones in the placenta: MRI was performed using a small animal MR scanner at 7.0T available at our institution (ClinScan). Isoflurane anesthetized mice were placed in prone position, and covered with a water-heated pad. Dynamic contrast-enhanced (DCE) MRI applying low molecular weight paramagnetic contrast agents (gadopentetatedimeglumine) was used to evaluate tissue perfusion. In brief, a dual-echo turbo-spin-echo (TSE) MR imaging sequences in coronal orientation was used to locate the placentas. A coronal three-dimensional T1-weighted gradient-echo sequence was acquired for T1 mapping by two different flip angles. For dynamic MR imaging, a similar three-dimensional T1-weighted gradient-echo sequence was used. Here, the second echo time was used for measuring and correcting transversal relaxation effects caused by high contrast agent concentrations.

*Histological analysis of the placenta*

Immunohistochemical detection of Proliferin, LYVE-1 and CEACAM-1 in placenta tissue sections (Suppl. Table 7):

Immunohistochemical detection was performed following established protocols (1,2). Briefly, for LYVE-1 and CEACAM-1 detection paraffin embedded tissue sections were deparaffinized, rehydrated and treated with 0.5 mg/ml Proteinase K (Roche) in TBS for 15 min at 37°C for epitope retrieval. Cryosections were used for Proliferin detection. Blocking steps were performed following the special needs for each protocol (Suppl. Table 7). Unspecific antibody binding was blocked by 30 min incubation with Protein Blocking Agent (Immunotech) or 10% swine serum in AB diluent (Dako). The slides were incubated overnight at 4°C with the primary antibody solution (Suppl. Table 7). After washing, sections were incubated for 1 h at room temperature with the secondary antibody solutions containing an antibody specific against the respective first antibody and subsequently washed. Tissue sections stained for LYVE-1 were incubated with avidin biotinylated alkaline phosphatase complex (Vector) 1% in TBS for 30 min, washed and incubated with a standard substrate solution containing neufuchsin (2), resulting in a pink signal. This was followed by light counterstaining with 0.1% Meyer's haematoxylin (Roth) and rinsing with tap water. Slides were directly mounted with a water based media. CEACAM-1 and proliferin positivity were detected by the fluorochrome conjugated to the secondary antibody. 4',6-diamidino-2'-phenylindole dihydrochloride (DAPI) was added in the last incubation step (Suppl. Table 7)

to counterstain nuclei, followed by mounting with the ImmuMount media. Sections were stored at 4°C for further analysis.

For light immunohistochemistry sections, image acquisition was performed using a slide scanner (Mirax Midi, Zeiss). Immunofluorescence sections were examined with a Zeiss Axioplan fluorescence microscope and pictures taken with the coupled RT slider spot camera.

The proportion of Proliferin<sup>+</sup> cells in a visual field was determined. Visual fields were randomly selected in zones of high positivity in the Junctional zone area. The number of LYVE-1<sup>+</sup> vessels per visual field was quantified manually using the Mirax Viewer. Since CEACAM-1<sup>+</sup> glycogen cells appear in clusters, CEACAM-1 was analyzed as CEACAM-1<sup>+</sup> area per junctional zone area. CEACAM-1 analysis required image processing and signal measurements that were performed with Adobe Photoshop CS3 (Adobe Systems) using the same settings for all images.

Parietal trophoblast giant cells (GC) quantification: The frequency of GC per area was calculated in Masson stained tissue sections. Only complete visible cells (nucleus + cytoplasm) were quantified. They were identified as large mononuclear cells whose nucleus had a diameter larger than 17 µm (3,4,5) due to their high ploidy and that were located between junctional zone and decidua.

Terminal deoxynucleotidyl transferase dUTP nick end labeling (TUNEL): The TUNEL assay was used as an indication of apoptotic cells in the placenta: Here, 10 µm cryostat sections of placental sections were freshly prepared and fixed in formalin, postfixed in ethanol/acetic acid, and incubated with digoxigenin-dUTP in the presence of terminal deoxynucleotidyltransferase (TdT), using a commercially available kit (Intergen). TUNEL-positive cells were visualized by anti-digoxigenin fluorescein isothiocyanate (FITC)-conjugated F(ab')<sub>2</sub> fragments, counterstaining was performed using DAPI dye (1 µg/ml methanol; Roche) in a subsequent incubation step. Finally, sections were mounted using VectaShield (Vector). Negative controls for the TUNEL staining were made by omitting TdT.

#### *Progesterone detection in urine samples*

Urine collection for hormonal analysis: Levels of progesterone were determined in urine samples of non-stressed control and stress challenged pregnant BALB/c females. This is a non-invasive method that parallels the fluctuations in serum (6). Urine samples were collected in the evening (6.30-7.30 pm) of gd 10.5 and daily from gd 12.5 to 15.5, which were consequently referred to as gd 11 and 13 to 16. At each time point, mice were placed individually on a net in a cage. After 15 min, each mouse was removed and urine was collected. Urine was stored at -20°C until hormone analyses were conducted simultaneously for all samples.

Progesterone and creatinine analysis in urine: Enzyme immunoassay (EIA) procedures were performed according to published protocols (6). Creatinine and progesterone were obtained from Sigma Chemical Co. An antibody to progesterone and corresponding horseradish peroxidase conjugate were obtained from the Department of Population Health and Reproduction at the University of California, Davis. The assay was carried out on antibody (1:10 000 in 50 mM bicarbonate buffer, pH 9.6) coated plates. For progesterone, urine samples were diluted 1:9 in phosphate buffer before they were added to the plate. Standard

curves were derived by serial dilution from a known stock solution. For all assays, 50  $\mu$ l of progesterone–horseradish peroxidase were added to each well, with 50  $\mu$ l of standard, sample, or control. The plates were incubated for 2 h at room temperature. Subsequently, the plates were washed and 100  $\mu$ l substrate solution of citrate buffer, H<sub>2</sub>O<sub>2</sub> and 2,20-azinobis (3-ethylbenzothiazoline-6-sulphonic acid) were added to each well and the plates were covered and incubated while shaking at room temperature for 30–60 min. The plates were then read with a single filter at 405 nm on the microplate reader (Bio-Tek Instruments).

It is common practice with urinary steroid analyses to compensate for variations in fluid intake and output by adjusting sample values for creatinine (6). Standard creatinine values were generated and urine samples diluted 1:50 in phosphate buffer (0.1 M; pH 7.0). DynatechImmulon flat bottom plates were used and 50  $\mu$ l per well of standard was added together with a solution 0.25 M NaOH and 0.13 M picric acid. The plates were incubated at room temperature for 30 min and subsequently measured for absorbance on a plate reader with a single filter at 490 nm. Standard curves were generated, regression lines were fit and the regression equation was applied to the optical density for each sample. Steroid measurements were adjusted for creatinine by dividing the obtained value by the measure of creatinine per ml of urine.

It should be noted that the standard curves for progesterone detection in urine by EIA and in serum by RIA are not identical and hence, a direct comparison of values should be avoided.

#### *Quantification of placental lactogen II, StAR and 3 $\beta$ HSD mRNA by Real Time RT-PCR*

RT-PCRs were conducted in Step One Plus Real-Time PCR Systems (Applied Biosystems) and the corresponding software using cDNA as template. Commercially available assays (Applied Biosystems) were employed for PCR amplification and detection of placental lactogen II (*Prl3b1*: Mm00435852\_m1) in the placental samples and StAR (*Star*: Mm 00441558\_m1) and 3 $\beta$ HSD (*HSD3b1*: Mm 01261921\_mH) in the ovaries. In the placenta HPRT was used as a housekeeping gene (Suppl. Table 2) whereas in the ovary  $\beta$ -Actin (*Actinb*: Mm 00607939\_s1) was selected. Every sample and target was run in triplicate. Quantification of the expression of the target gene in relation to the respective housekeeping gene was carried out employing the “Comparative ( $\Delta\Delta$ ) CT Method”.

#### *Placental cell isolation*

Fresh placental tissue was detached from the decidua and uterus, mechanically minced and mashed through a 40  $\mu$ m cell strainer. After washing with PBS placental cell suspensions were further depleted of erythrocytes by incubating with the RBC lysis buffer (e-Bioscience). Cells were washed with PBS and re-suspended in FACS buffer (0.5% BSA in PBS). Cell viability and concentration was assessed by counting the Trypan blue negative cells in a hemocytometer. Cell suspensions were stained according to our previously protocol and immune cell phenotype and HMOX-1 expression was analyzed by flow cytometry.

## Supplemental tables

Supplemental table 1: List of antibodies used to perform the FACS analysis of leukocytes isolated from inguinal lymph node tissue.

Antigen Specificity	Fluorochrome	Clone	Dilution	Company/catalog number
CD3e	APC	145-2C11	1:200	Biolegend/100311
CD279	FITC	J43	1:200	eBioscience/11-9985-82
CD122	PE	TM- b1	1:200	eBioscience/12-1222-81
CD28	PerCP-Cy5.5	37.51	1:200	eBioscience/45-0281-82
CD11c	PE-Cy7	HL3	1:200	BD Pharmingen/558079
CD8a	Pac Blue	53-6.7	1:200	Biolegend/100725
CD4	APC	RM4-5	1:200	BD Pharmingen/553051
CD25	PE-Cy7	PC61	1:200	BD Pharmingen/552880
Foxp3	PerCP-Cy5	FJK-16s	1:200	eBioscience/45-5773-80
CD49b	FITC	DX5	1:200	BD Pharmingen/553857
MHCII	FITC	14-4-4S	1:200	BD Pharmingen 553543
HO-1	PE	HO-1-2	1:100	Abcam/ab83214
CD11b	PerCP-Cy5.5	M1/70	1:200	BD Pharmingen/550993

Supplemental table 2: List of primers (TibMolbiol) used for mouse genotyping.

<i>Hmox1</i>	Wildtype Primer Forward (19mer)	5'-GGTGACAGAAGAGGCTAAG-3'
	Wildtype Primer Reverse (19mer)	5'-CTGTA ACTCCACCTCCAAC-3'
	Mutant Primer Forward (20mer)	5'-TCTTGACGAGTTCTTCTGAG-3'
	Mutant Primer Reverse (19mer)	5'-ACGAAGTGACGCCATCTGT-3'
<i>Pgr</i>	Wildtype Primer Forward (20mer)	5'-AGCCACTCATAGGGAGGGAG-3'
	Wildtype Primer Reverse (20mer)	5'-GTCGCCGTAAGAGGGAACA-3'
	Mutant Primer Forward (20mer)	5'-CAAGATGGATTGCACGCAGG-3'
	Mutant Primer Reverse (19mer)	5'-TGATATTCGGCAAGCAGGCA-3'

Supplemental table 3: Primers and probe used for *Hprt* qRT-PCR gene expression quantification

<i>Hprt</i> F-primer (24mer)	5'- ggAATTTgAATCACgTTTgTgTCA -3'
<i>Hprt</i> R-primer (24mer)	5'- TTTTACTggCAACATCAACAggAC -3'
<i>Hprt</i> probe	5'- 6FAM-TTgCAgATTCAACTTgCgCTCAXTCTT-PH -3'

Supplemental table 4: *Hmox1* pyrosequencing assay. Overview of the mouse *Hmox1* promoter.

Mouse <i>Hmox1</i> promoter	
GGGCC <u>CG</u> CCTC <u>CG</u> GGCTGGATGTTGCAACAGCAG <u>CG</u> AGAA <u>CG</u> <u>CG</u> GCTCAGCTGGG <u>CG</u> GCCACCA <u>CG</u>	1 2 3 4 5 6 7
	<b>TSS</b>
TGACC <u>CGCG</u> TACTTAAAGGGCTGG <u>CGCG</u> GGCAGCTGCT <u>CG</u> CTCA <u>CG</u> GTCTCCAGT <u>CG</u> CCTCCAGAGT	8 9 10 11 12 13 14
TTC <u>CG</u> CATAACAACCAGTGAGTGGAGCCTGCC <u>CGCG</u> CAGAGC <u>CG</u> TCT <u>CG</u> AGCATAGCC <u>CG</u> GAGCCTGA	15 16 17 18 19 20
AT <u>CG</u> AGCAGAACCAGCCTGAACTAGCCCAGT <u>CG</u> GTGATGGAG <u>CG</u> TCCACAGCC <u>CG</u> ACAGGCAAG <u>CG</u>	21 22 23 24 25

Numbering of CpG positions is according to Zhao et al. (7). TSS refers to the transcription start site. The grey-shadowed sequence corresponds to a response element for Sp-1.

Supplemental table 5: *Hmox1* pyrosequencing assay. Primers used for *Hmox1* PCR:

Part 1	<i>Hmox1</i> F-primer	5'- GGTAGGTTTTATTTATTGGT -3'
	<i>Hmox1</i> R-primer	5'- CTCCCTTTTTTTTTATAACAAACTTACC (biotin)-3'
Part 2	<i>Hmox1</i> F-primer	5'- TGGTTTTGTAGTTTTGTATTTTTAGGTAGGA -3'
	<i>Hmox1</i> R-primer	5'- GGTAGGTTTTATTTATTGGTTGTATGTGGA (biotin) -3'

Supplemental table 6: *Hmox1* pyrosequencing assay. Primers used for sequencing:

CpG position	Sequence	Sequence-to-analyze
25-22*	GTTATAGTTTTTTTTTTATATA GT	YGTTTGTGGTGGAYGTTTATTATYGGATTG
21-16	GGGTTAGTTTAGGTTGG	TTTTGTTYGATTAGGTTYGGTTATGTYGAGAYGGTTTG YGGGTAGGTTTATTTATGTTG
15-10	GGTAGGTTTTATTTATTGGT	TGTATGYGGAATTTGGAGGYGATTGGAGATYGTGAGYGAG TAGTTGTYGYGTTAGTTTTTAAGTA
11-6	GATAGTGAGAGAGTAGTTGT	TYGYGTTAGTTTTTAAGTAYGYGGTTAYGTGGTGGTYGTT AGTTGAGT
5-1	TGGTGGTAGTTTAGTTGAG	TYGGYGTTTYGTTGTTGTTGTAATATTAGTYGGAGGYGGG TTTTGTTGTAAGGGGATAAATTA

\* we were unable to obtain reliable methylation data for position CpG23

A red T refers to C nucleotides in the unconverted original DNA sequence. Y denotes C or T nucleotides after bisulfite conversion, indicating mC or C in the original sequence.

Supplemental table 7: Immunohistochemical staining protocol features of placental tissue sections.

Part 1:

Antigen Detection	Tissue	Antigen retrieval	Blocking		First AB against (1); (dilution)	Cat N°
Proliferin	cryosections	-	-	Avidin, biotin and protein block	Goat $\alpha$ -mouse (0.5 % in 1% FCS TBS)	sc-47345 Sta. Cruz
HMOX-1			PO blocking		Rabbit $\alpha$ -mouse (1 % in 1% FCS TBS)	ab68477 Abcam
CD34	Paraffin sections	citrate buffer	10 % swine normal serum in AB diluent		Rat $\alpha$ -mouse (10 % in AB diluent)	Ab8158 Abcam
LYVE-1		Proteinase K			Biot. goat $\alpha$ -mouse (3.3 % in AB diluent)	BAF2125 R&D
CEACAM-1					Rabbit $\alpha$ -mouse (0.1 % in AB diluent)	(B)

## Part 2:

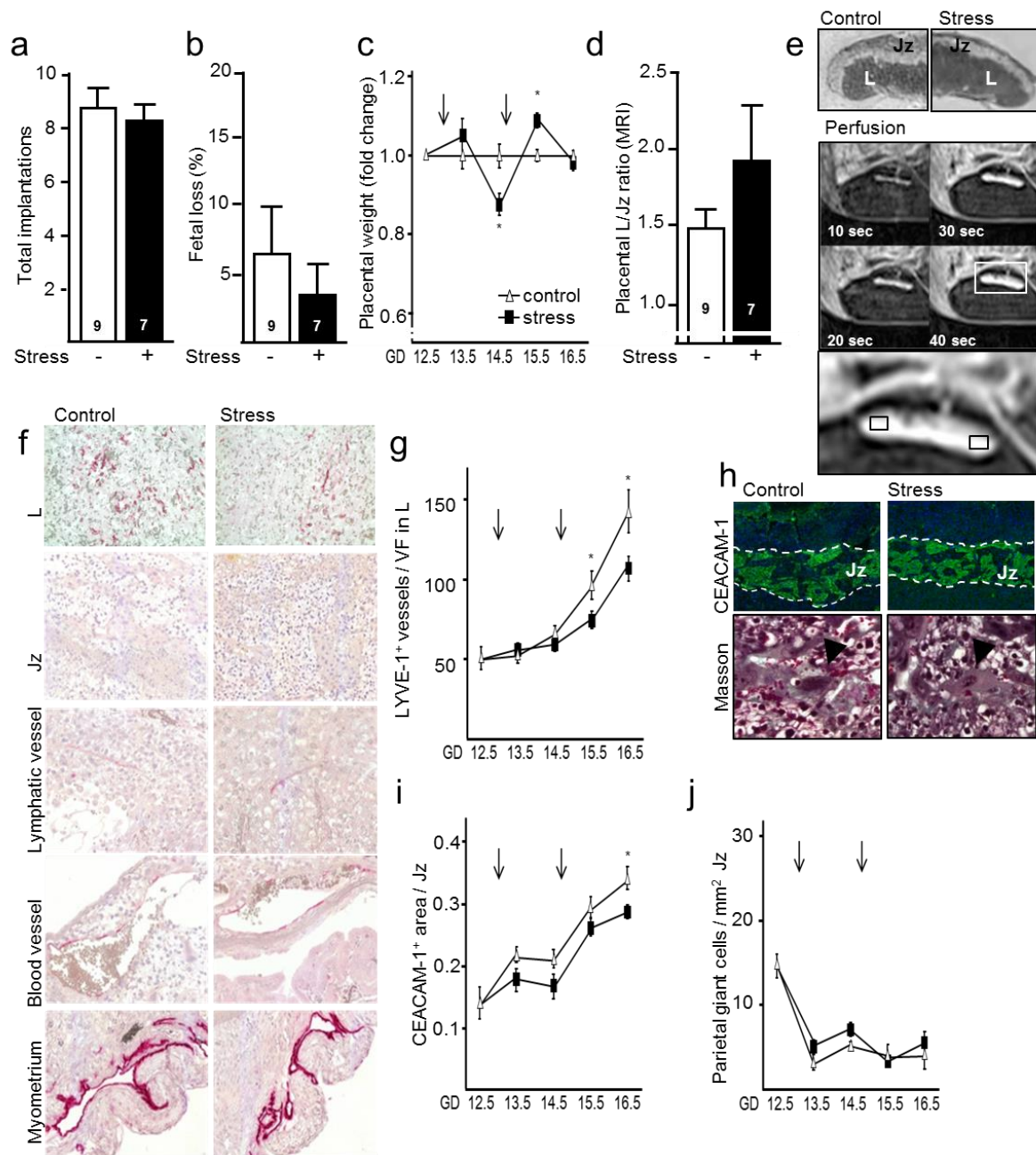
Antigen Detection	Secondary AB; (dilution)	Amplification/ detection	Mounting media
Proliferin	TRITC-donkey $\alpha$ -goat IgG (0.5 %) + DAPI in (A)	-	Immu-Mount media
HMOX-1	Biot. goat $\alpha$ -rabbit IgG (0.5 %) in (A)	ABC-PO/ DAB+H <sub>2</sub> O <sub>2</sub>	Vitroglut
CD34	Biot. rabbit $\alpha$ -rat IgG (0.5 %) + DAPI in AB diluent	Streptavidin-Cy3	Immu-Mount media
LYVE-1	-	ABC-AP/ neufuchsin	Clear mounting media
CEACAM-1	AF 488 donkey $\alpha$ -rabbit IgG (0.5 %) + DAPI in AB diluent	-	Immu-Mount media

(A) 2% FCS 4% MNS TBS

(B) Rabbit  $\alpha$ -mouse CEACAM-1 AB was prepared as described before (1)

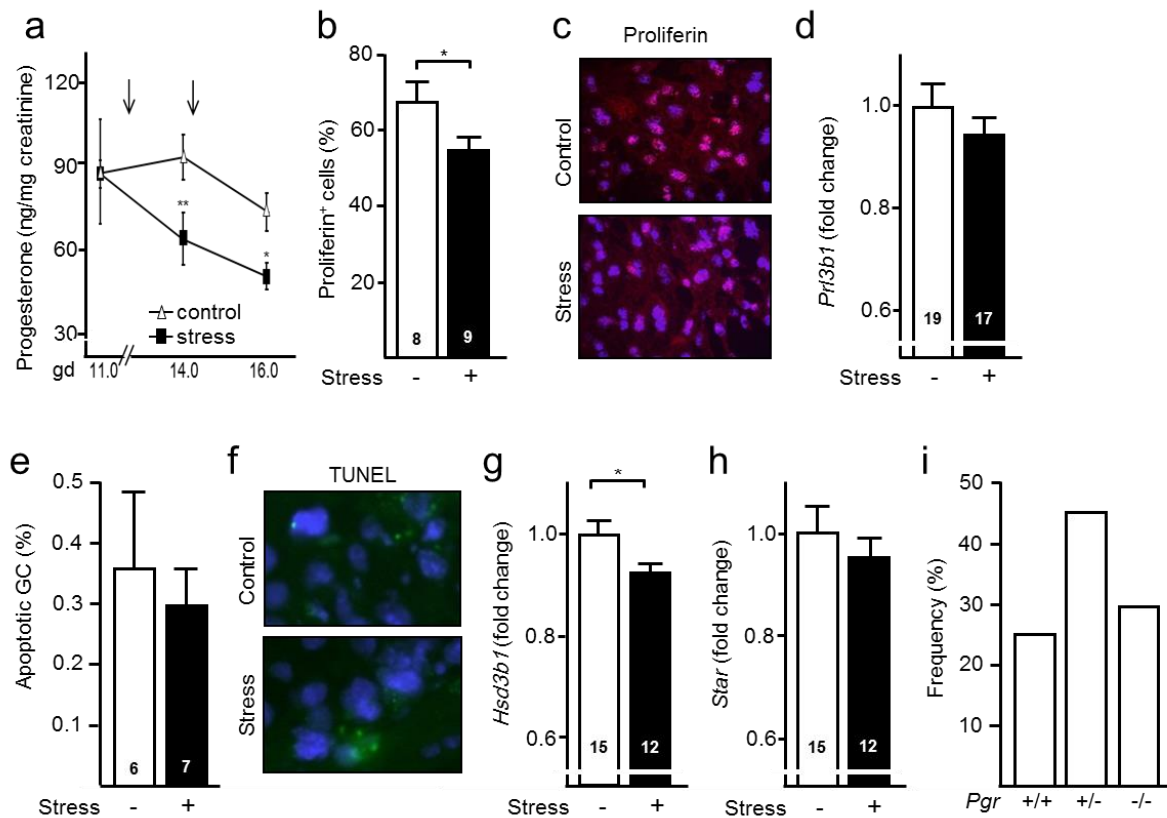
All secondary antibodies were purchased in Jackson ImmunoResearch.

## Supplemental Figures

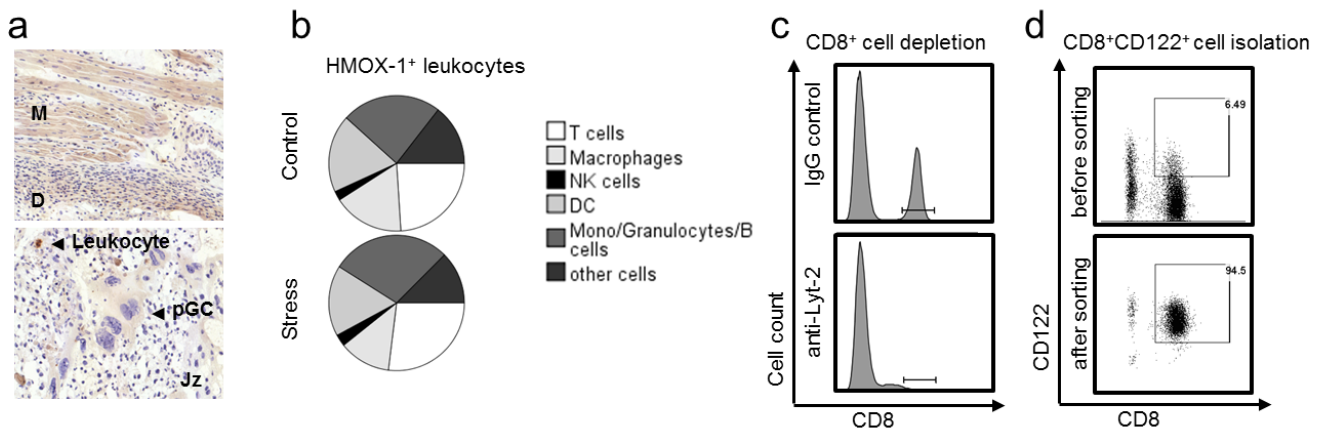


**Supplemental figure 1: Mid-gestational stress challenge induced morphological changes in the placenta.** Stress challenge did not affect litter size (a) or fetal loss rate (b). Placental weight was evaluated in control and stress-challenged dams between gd 12.5 and 16.5 as an indicator for placental growth (c). Placental weights of stress-challenged animals were normalized to the control group for the respective gd. (d) 3D MRI evaluation of placental tissue on gd 16.5 confirmed the increase in the L/Jz ratio observed in histological analysis. MRI permitted to correct the angle of the placental tissue, thereby decreasing the technical error associated to histological sectioning and increasing the level of significance. (e) Representative images of the MRI scans generated for analysis. Top: control and stress-challenged placentas scanned ex vivo by MRI. Jz can be distinguished from L by its higher uptake of contrast enhancer. Bottom: MRI was further employed to identify the areas of high blood perfusion in the labyrinth, optimal for CD34<sup>+</sup> fetal vessel

density quantification. Photos were taken 10, 20, 30 and 40 sec (top to bottom, left to right) after i.v. administration of contrast enhancer (white). The photo in the bottom shows a magnification of the placenta at 40 sec (white rectangle). The highest perfusion (black rectangles) occurred in distal areas where the flow was unaffected by the central arterial placental canal or the chorionic plate vessels. (f) Additional characterization of the placenta revealed the expression of LYVE-1 in mouse placenta. LYVE-1 is generally expressed in lymphatic vessels and in human syncytiotrophoblast cells during late pregnancy (8). From top to bottom, LYVE-1<sup>+</sup> vessels were enriched in the lateral areas of the labyrinth and in the proximity of the junctional zone, whereas the staining was negative in the junctional zone, faint in lymphatic (not containing erythrocytes) and blood (containing erythrocytes) vessels in the decidua, and positive in vessels in the myometrium (magnification 200 x). There were no differences among groups in LYVE-1<sup>+</sup> vessels in decidua (data not shown), whereas the positivity in the myometrium could not be quantified because of the direction in which the tissue was embedded. (g) The frequency of LYVE-1<sup>+</sup> vessels within the vascular net of the labyrinth increased over gestation and, starting on gd 15.5, it was significantly reduced in response to the stress challenge. Interestingly, LYVE-1 expression in the labyrinth does not appear to be associated to lymphatic drainage of the placenta, as there was no evidence for LYVE-1<sup>+</sup> vessels in the junctional zone. Next, we analyzed the junctional zone from control and stress challenged placentas, thereby focusing on CEACAM-1<sup>+</sup> cells and the parietal trophoblast giant cells (h). Top: Similar to the expression in extravillous trophoblast cells in human placentas (9) CEACAM-1 (green; cell nuclei appear in blue) can be used as a marker facilitating the identification of glycogen trophoblast cells. Bottom: parietal giant cells were analysed in Masson stained tissue sections. Magnification: 50 x (top) and 200 x (bottom). (i) The ratio of CEACAM-1<sup>+</sup> to junctional zone areas was significantly decreased in stress-challenged tissue compared to controls. However, no differences in the parietal trophoblast giant cells (pGCs) numbers were observed in tissues from control and stress-challenged pregnancies on gd 12.5 to 16.5 (j). Abbreviations: Lymphatic vascular endothelial hyaluronan receptor-1: LYVE-1; carcinoembryonic antigen-related cell adhesion molecule-1: CEACAM-1. Graphs represent the mean  $\pm$  SEM per group. Arrows in (c,h,j,k) indicate the beginning of the 24 h exposition to sound stress (gd 12.5 and 14.5). \* denotes  $p \leq 0.05$ , \*\* refers to  $p \leq 0.01$ , obtained by the Mann Whitney U Test. In the histological analysis, a minimum of 8 placentas per group and gd were quantified to identify differences between control and stress-challenged groups.



**Supplemental figure 2: low progesterone levels induced by stress are associated to a decrease expression of progesterone synthesizing enzymes in the ovary.** As was observed in serum analyses, progesterone was reduced in urine samples (a) of stress-challenged dams on gd 14 and 16, when compared to controls (control group n=7 in gd 14 and n=5 in gd 16; stress challenged group n=8 in gd 14, n=6 in gd 16). (b) Frequency of Proliferin<sup>+</sup> cells in Jz area, identified by immunofluorescence. (c) Representative photomicrographs in support of data shown in (b) on Proliferin expression in Jz; Proliferin<sup>+</sup> cells appear in red, cell nuclei were detected by DAPI (blue); magnification 200 x. (d) Placental lactogen II - *Prf3b1*- gene expression was quantified by RT-PCR. (e) Proportion of apoptotic giant cells, as identified by its positivity for TUNEL assay. (f) Photomicrographs of an apoptotic body (bright green) illustrated the data shown in (e); cell nuclei appear in blue; magnification 400 x. RT-PCR analyses revealed a decrease in the expression of 3 $\beta$ HSD -*Hsd3b1*- (g) upon stress, as well as a non-significant reduction of StAR -*Star*- (h). *Pgr*<sup>+/-</sup> matings resulted in litters exhibiting a Mendelian-like distribution for the *Pgr* genotype (i). Graphs represent the mean  $\pm$  SEM per group. Arrows in a indicate the beginning of the 24 h exposition to sound stress (gd 12.5 and 14.5). \* denotes  $p \leq 0.05$ , \*\* refers to  $p \leq 0.01$ , obtained by the Mann Whitney U Test.



**Supplemental figure 3.** (a) Immunohistochemistry staining of gd 16.5 placentas revealed that HMOX-1 was expressed in the myometrium (M), decidua (D), in leukocytes infiltrating the placenta (arrow) as well as in the cytoplasm of parietal trophoblast giant cells (pGC). (b) Flow cytometric characterization of HMOX-1<sup>+</sup>CD45<sup>+</sup> leukocytes isolated from control and stressed placental tissue. (c) Representative histograms show CD8 positivity in cells obtained from the uterus draining lymph nodes of females treated with anti-Lyt 2 antibody to achieve the depletion of CD8<sup>+</sup> cell, or the corresponding IgG control. (d) Representative dotplots showing the purity of CD8<sup>+</sup>CD122<sup>+</sup> cells before and after flow cytometric sorting.

## References

---

1. Horst AK, Bickert T, Brewig N, Ludewig P, van Rooijen N, Schumacher U, Beauchemin N, Ito WD, Fleischer B, Wagener C, Ritter U. CEACAM1+ myeloid cells control angiogenesis in inflammation. *Blood*. 2009;113(26):6726-36.
2. Solano ME, Sander VA, Ho H, Motta AB, Arck PC. Systemic inflammation, cellular influx and up-regulation of ovarian VCAM-1 expression in a mouse model of polycystic ovary syndrome (PCOS). *J Reprod Immunol*. 2011;92(1-2):33-44.
3. Simmons DG, Rawn S, Davies A, Hughes M, Cross JC. Spatial and temporal expression of the 23 murine Prolactin/Placental Lactogen-related genes is not associated with their position in the locus. *BMC Genomics*. 2008;28;9:352.
4. Cross JC. How to Make a Placenta: Mechanisms of Trophoblast Cell Differentiation in Mice – A Review. *Placenta*. 2005;26 Suppl A:S3-9.
5. El-Hashash AH, Kimber SJ. Trophoblast differentiation in vitro: establishment and characterisation of a serum-free culture model for murine secondary trophoblast giant cells. *Reprod*. 2004;128(1):53-71.
6. deCatanzaro D, Muir C, Beaton E, Jetha M, Nadella K. Enzyme immunoassay of oestradiol, testosterone and progesterone in urine samples from female mice before and after insemination. *Reproduction*. 2003;126(3):407-14.
7. Zhao H, Wong RJ, Nguyen X, Kalish F, Mizobuchi M, Vreman HJ, Stevenson DK, Contag CH. Expression and regulation of heme oxygenase isozymes in the developing mouse cortex. *Pediatr Res*. 2006 ;60(5):518-23.
8. Gu B, Alexander JS, Gu Y, Zhang Y, Lewis DF, Wang Y. Expression of lymphatic vascular endothelial hyaluronan receptor-1 (LYVE-1) in the human placenta. *Lymphat Res Biol*. 2006 Spring;4(1):11-7.
9. Bamberger AM, Sudahl S, Löning T, Wagener C, Bamberger CM, Drakakis P, Coutifaris C, Makrigiannakis A. The adhesion molecule CEACAM1 (CD66a, C-CAM, BGP) is specifically expressed by the extravillous intermediate trophoblast. *Am J Pathol*. 2000;156(4): 1165-70.